Full Paper Transactions, SMiRT 28
Toronto, Canada, August 10-15, 2025

IMPACT TESTS TO STUDY THE EFFECT OF AGGREGATE GRAIN SIZE ON THE BALLISTIC RESISTANCE OF CONCRETE

Ari Vepsä[1]

[1] Senior Scientist, VTT Technical Research Centre of Finland, Espoo, Finland (ari.vepsa@vtt.fi)

INTRODUCTION

Aircraft impact is one of the external threats for the integrity of nuclear power plants. While the fuselage of an aircraft may cause large displacements and strains in the reinforcement of the structures, in the worst-case hard parts of the aircraft may perforate the structure. The effect of different parameters on the ballistic limit of concrete slabs under hard projectile impacts has been studied for example at VTT in the multinational Impact projects (Orbovic et al., 2105). However, a parameter, which has been omitted in the test series due to limited resources is the maximum grain size of the concrete used.

It has been known for a long time that increasing the size of the aggregates decreases the tensile strength of concrete as well as its limit of elongation (Tsiskreli ansd Dzhavakhidze, 1970). However, its possible effect has been ignored in most of the formulas concerning perforation resistance of concrete slabs. Whiffen (1943) assumed that the penetration depth, x, is dependent on the aggregate size, a, as shown in Equation 1:

$$\frac{x}{d} \propto \left(\frac{d}{a}\right)^{0.1} \tag{1}$$

where d is the projectile diameter, so that doubling of the aggregate size decreases the penetration depth by 7 %. Kar (1978) took the grain size into account in the expression for perforation limit, e, as follows:

$$\frac{e-{}^{a}/_{2}}{d} = f\left(\frac{x}{d}\right) \tag{2}$$

where $f(x/d)$ is a function of x/d. According to equation 2, increasing the size of the aggregate also increases the perforation limit and therefore decreases the perforation resistance. It can also be seen that the effect of the grain size is rather small, that it decreases as the perforation limit increases and that it increases (in relation) when the grain size increases.

To investigate the effect of this parameter further, two tests were carried out by VTT by varying the maximum grain size (8 mm & 32 mm) and using only plain concrete without reinforcement at the impacted area. As most of the formulas for perforation limit and thus ballistic limit take only the compression strength of concrete as an input value, the aim was to keep the compressive strength of the two batches of concrete as close to each other as possible.

METHODS

The tests were conducted with 2.1 *2.1*0.25 m concrete slabs having the maximum grain sizes of 8 mm and 32 mm. The slabs were reinforced only on the edges with D10 rebars having spacing of 90 mm. The impacted area (630 mm * 630 mm at the front, 1170 mm * 1170 mm at the rear) was left unreinforced. The secondary goal of the tests was to validate the concrete material models used in numerical simulations. This is easier to achieve when the combined effect of concrete and reinforcement is eliminated.

The slabs were impacted with 47.6 kg carbon steel projectiles shown in Figure 1. The impact velocities, v_0, realized in the tests were 104.9 m/s for the slab with max 8 mm aggregates and 104.0 m/s for the slab with max 32 mm aggregates. The tests were recorded with high shutter speed video cameras to determine the residual velocity, v_r, of the projectile after perforation. The projectiles had an aluminium "tail" at the rear which was still visible from the front side when the nose of the projectile had perforated the slab and which thus enabled determination of the residual velocity.

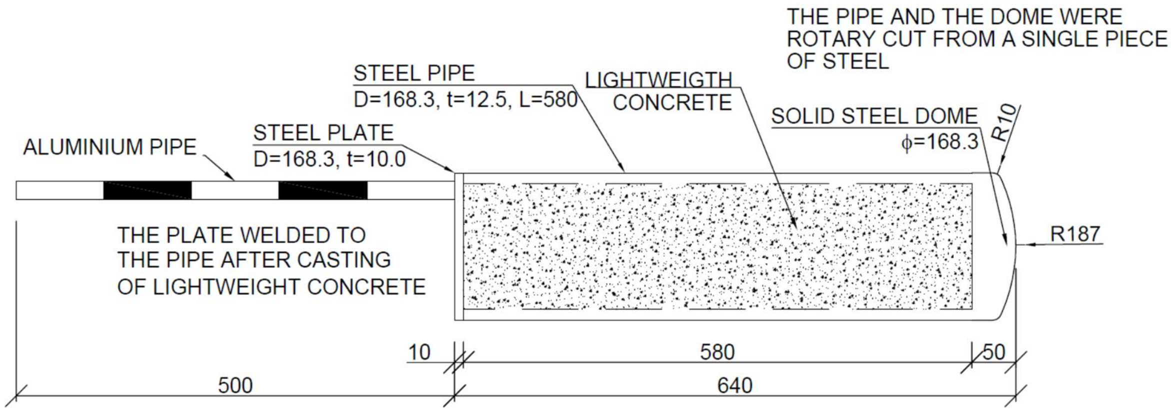

Figure 1. Hard projectile used in the test.

The impact tests were carried out with an old impact test apparatus of VTT, shown in Figure 2. The apparatus used pressured air to drive the projectile towards the target and it consisted of two parts: the pressure accumulator tube and the launch tube. The projectile is placed on rails that are attached on top of the launch tube while a piston shaped steel structure is placed inside the tube. This piston structure has a fin which protrudes up from the tube through an axial split that runs throughout its whole length. The piston is pushed forward by compressed air, released to the launch tube, and the fin of the piston pushes the projectile. The piston is caught with a separate steel structure in front of the launch tube before it hits the target while the projectile continues its flight and hits the target.

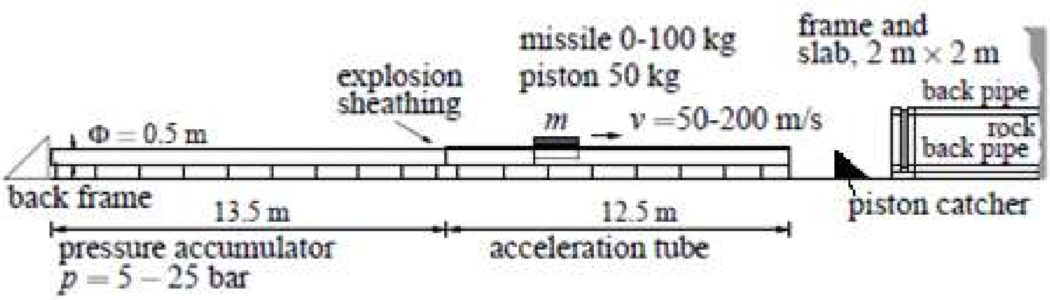

Figure 2. VTTs old impact testing apparatus.

The target slabs were attached between two halves of a steel frame. The frame was then erected and attached to 4 steel support pipes. The other end of the pipes was attached to the rear wall of the facility. The support forces acting on the pipes during the test were determined from strain gauge measurements made on the pipes.

The masses of water, m_w, aggregates, m_{ag}, cement, m_{cem}, and fly ash, m_{fa}, used for both batches of concrete are collected in Table 1 per m^3 of concrete. The mass of aggregates is presented separately for the grains smaller than 8 mm and those larger than 8 mm. The batches of concrete were tested for unconfined compressive strength, measured with both cubes, $f_{c,c}$, as well as with cylinders, $f_{c,Cyl.}$, splitting tensile strength, f_{ct}, Young's modulus, E, and Poisson's ration, ν. Splitting tensile strength testing was carried out using five quasi-static loading velocities (0.2, 2, 20 ,100 and 200 kN/s) to check whether the different batches of concrete have also different response to increased loading velocity. The tested cube samples were the size of 150 mm while the cylinder samples were the size of h300 mm and d150mm, except for the splitting tensile strength samples, which were the size of h200mm and d100mm. The material test results are summarized in Table 2, except for the splitting tensile strength results which are presented in Figure 3. For the figure, the loading velocity was converted to average strain rate. As can be seen, there was no remarkable difference between the batches of concrete in their response to the increase in the loading velocity.

Table 1. Mass of adhesives and aggregates used for the concrete batches.

Test no.	*Max. a*	ρ	m_w	$m_{cem.}$	m_{fa}	$m_{ag(\leq 8mm)}$	$m_{ag(8...32mm)}$
	mm	*kg/m³*	*kg/m3*	*kg/m3*	*kg/m3*	*kg/m³*	kg/m³
1	8	2265	243	411	116	1521	-
2	32	2322	186	364	103	984	750

Table 2. Concrete material test results

Test no.	*Max. a*	f_c	$F_{c,Cyl.}$	E	ν
	mm	*MPa*	*MPa*	Mpa	–
1	8	57.5	51.8	30.16	0.207
2	32	57.5	49.9	32.26	0.202

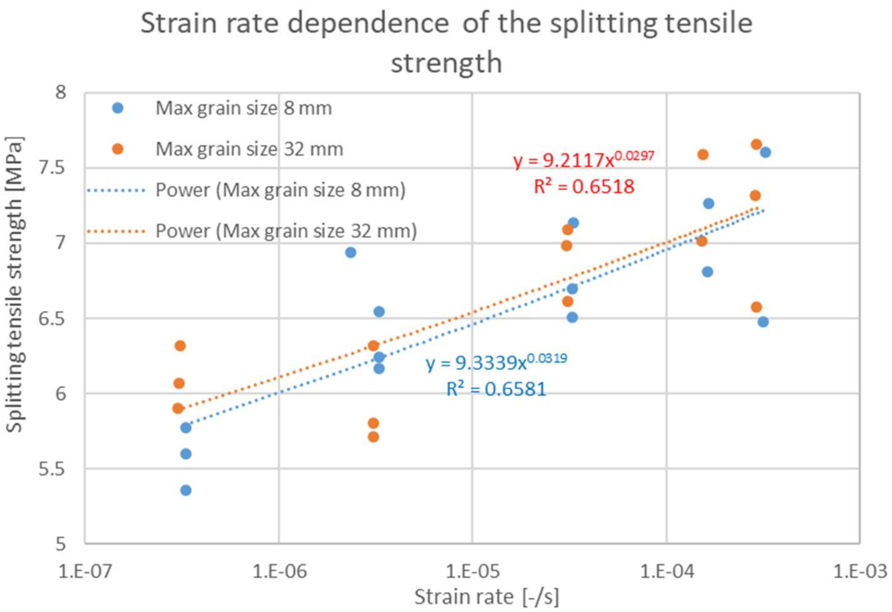

Figure 3. Splitting tensile test results.

After the tests, the mass of the concrete detached from the slabs, m_c , was measured. The ballistic limit of the slabs, v_p, was computed from the test results in accordance with energy balance using the Kar formula (Equation 3), (Kar, 1979):

$$\frac{1}{2}m_p v_0^2 = \frac{1}{2}m_p v_p^2 + \frac{1}{2}(m_p + m_c)v_r^2, \tag{3}$$

where m_p is the mass of the projectile. The equation assumes that the concrete detaches as a single plug with the same velocity than that of the projectile after perforation. However, in reality the concrete is broken in such a hard impact into small particles with each having slightly different velocity that also differs from the residual velocity of the projectile. The higher the mass of the detached concrete, the larger the effect of the assumption made on its ejection velocity.

TEST RESULTS

The main results of the impact tests are summarized in Table 3. The data shown includes the maximum grain size, the mass of the concrete detached, the residual velocity of the projectile, the ballistic limit of the target slab, the area of the spalled concrete on the front surface of the target, A_{sp}, and the area of the scabbed concrete on the rear surface of the target, A_{sc}.

Table 3 Test results.

Test no.	a	v_0	m_c	v_r	v_p	A_{sp}	A_{sc}
	mm	m/s	Kg	m/s	m/s	m^2	m^2
1	8 mm	104.9	66.8	42	**82**	0.09	0.52
2	32 mm	104.0	141.3	49	**36**	0.12	0.89

Still pictures from the high shutter speed video material are shown in Figure 4. The frames have been taken roughly 2.8 ms apart starting at the moment of impact. The frames on the upper and third row are from the test 1 with the smaller maximum grain size and the frames on the second and last row from the test 2 with the larger maximum grain size.

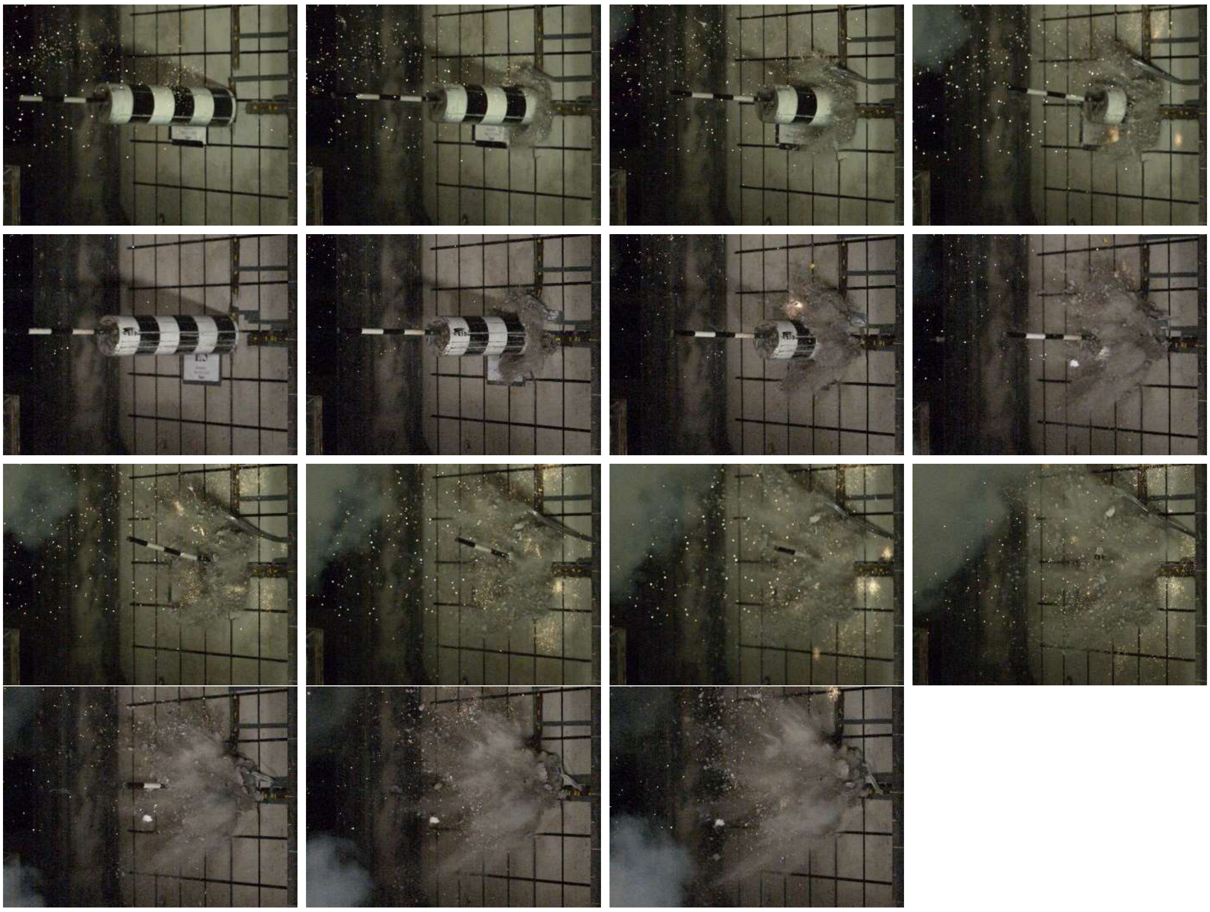

Figure 4. Still pictures from the high shutter speed video material. Rows 1 and 3: test 1. Rows 2 and 5: test 2.

The dependence between the ballistic limit and the concrete ejection velocity is studied for both slabs in Figure 5. Here a unified ejection velocity is assigned for all the concrete particles in both tests. The dots in the graph mark the “actual” ballistic limits of the slabs, obtained assuming that the ejection velocity is the same than the projectile residual velocity. Even if this assumption didn’t not hold true and the actual ejection velocities were lower, the ballistic velocity would be lower for the slab with a=32 mm than for the slab with a=8 mm.

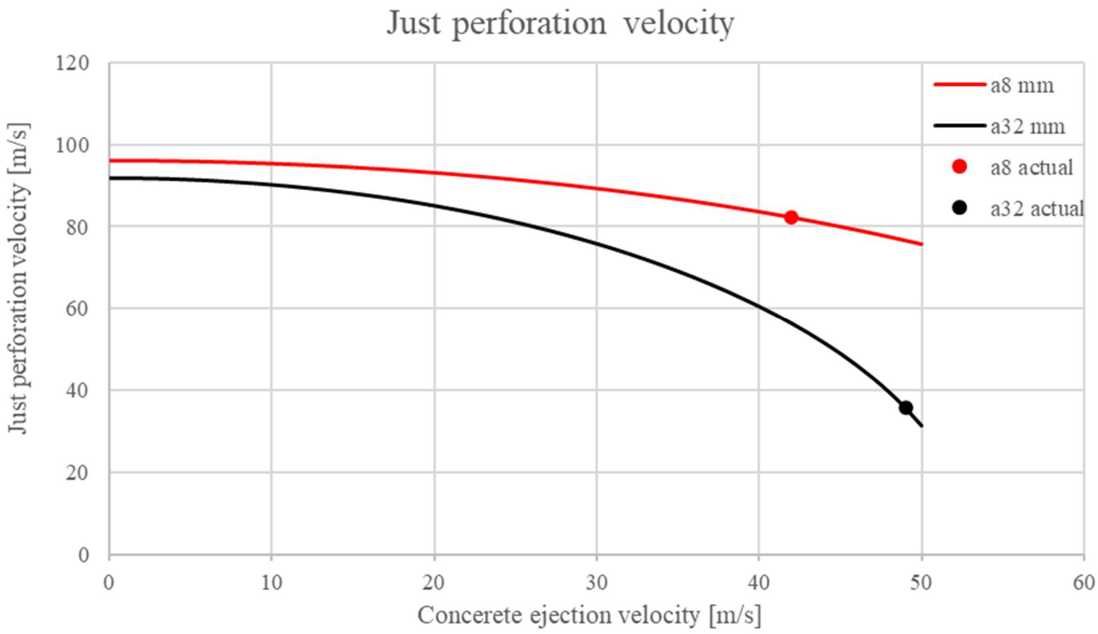

Figure 5. Dependence between the just perforation velocity and the concrete ejection velocity.

The rear faces of the tested slabs are shown in Figure 6 after the test. The slabs were sawn into quartiles after the test. The sawn horizontal cross-sections of the slabs are shown in Figure 7. The dashed red lines in Figure 6 indicate these cross-sections. Close up of the rear surface of slab 2 is shown in Figure 8. Big part of the largest aggregates has been detached from the surrounding medium, leaving light grey holes at their place in the cement paste. Some of the largest aggregates are shown in Figure 9. As can be seen, these are relatively rounded and smooth in shape.

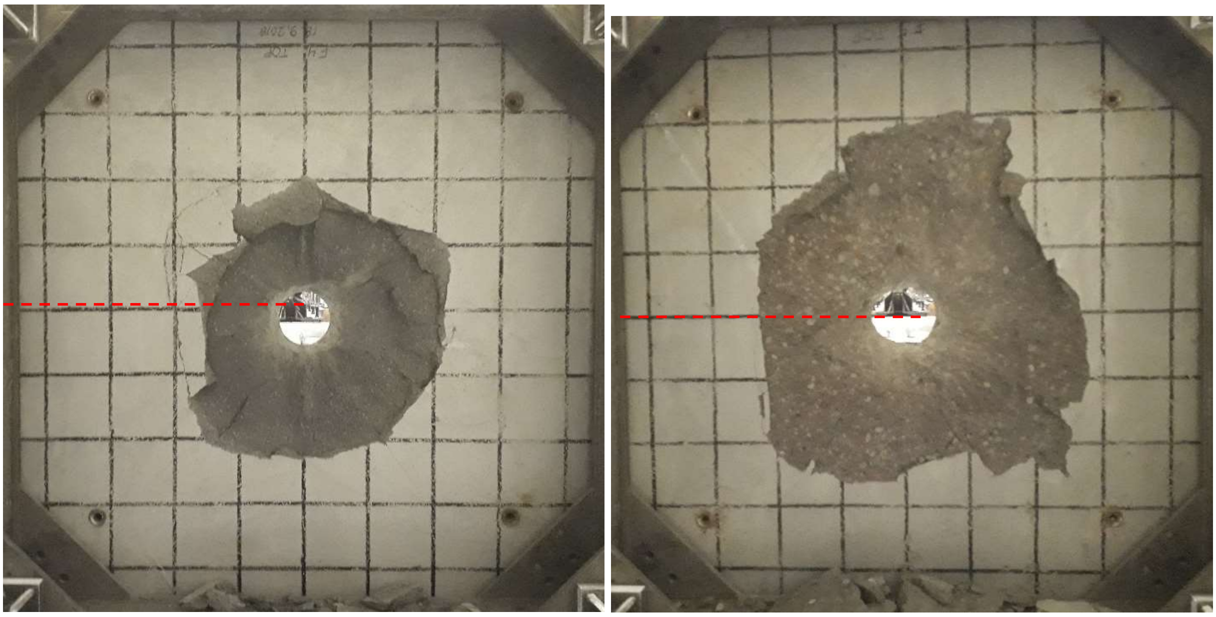

Figure 6. Rear face of the tested slabs after the tests.

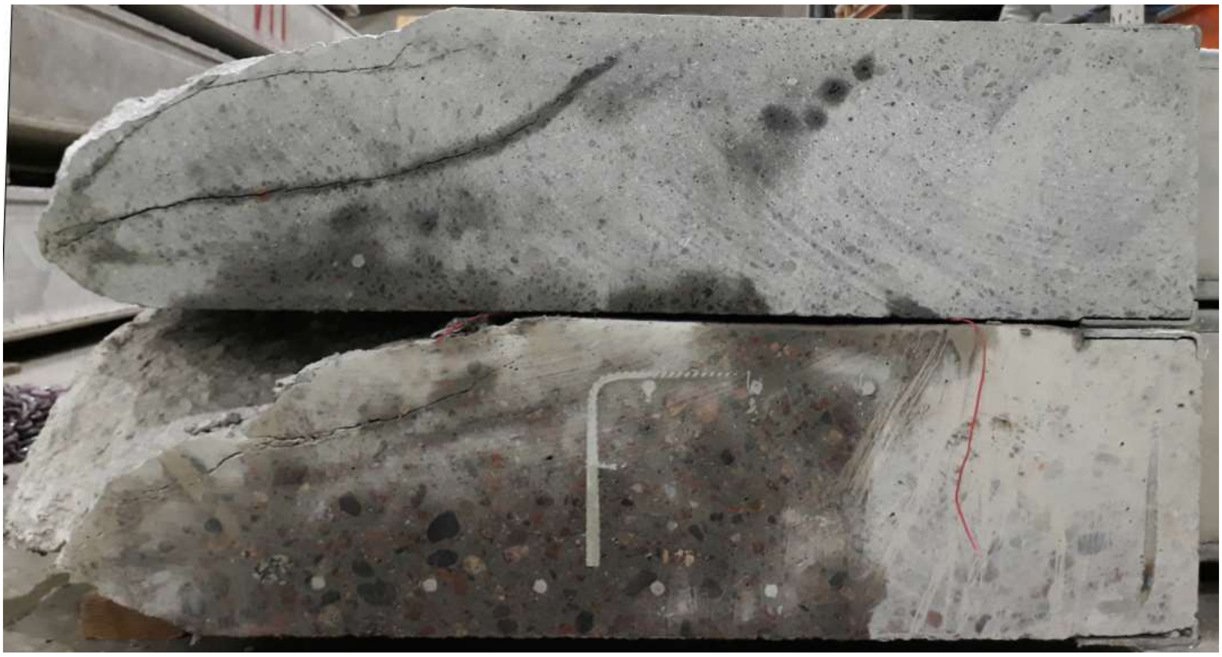

Figure 7. Sawn horizonal cross-sections of the tested slabs.

Figure 8. Close-up of the rear surface of slab 2 after the test.

Figure 9. Some of the largest aggregates of concrete batch 2.

The total force acting on the supports is shown on the left in Figure 10. The impulse integrated from them is shown on the right together with the change of momentum of the projectile.

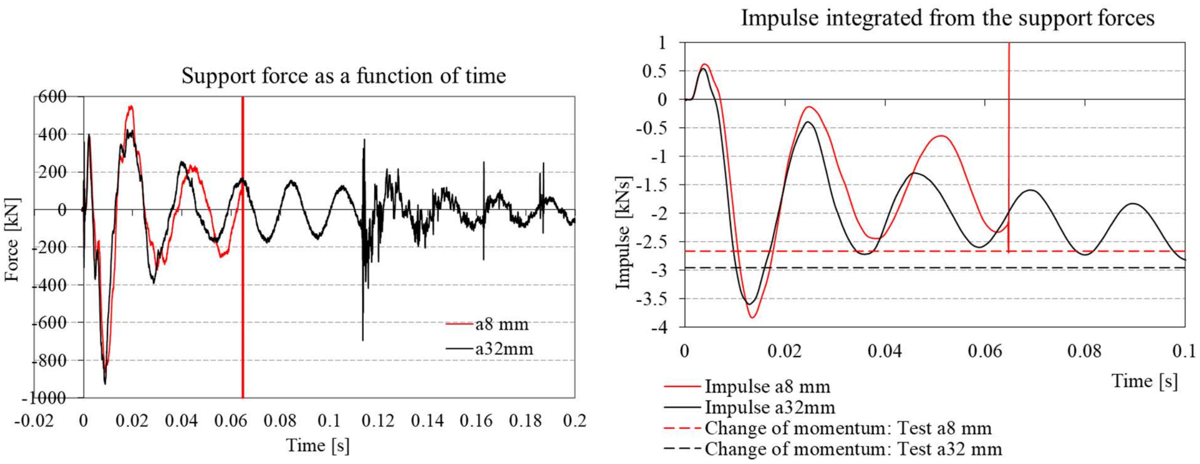

Figure 10. Total force acting on the supports in tests 1 and 2 (left) and the impulses integrated from these forces together with the reduction of the momentums of the projectile during the tests (right).

The largest detached concrete particles were weighed after the test. The weight distributions of the particles are shown in Figure 11. The particles of concrete with the larger aggregates were considerably larger than the one with the smaller aggregate size. It should also be noted that some of the particles have broken into smaller pieces when they hit the surrounding structures of the facility and not during the impact. It can also be seen that in both cases, majority of the detached concrete was broken into very small fragments.

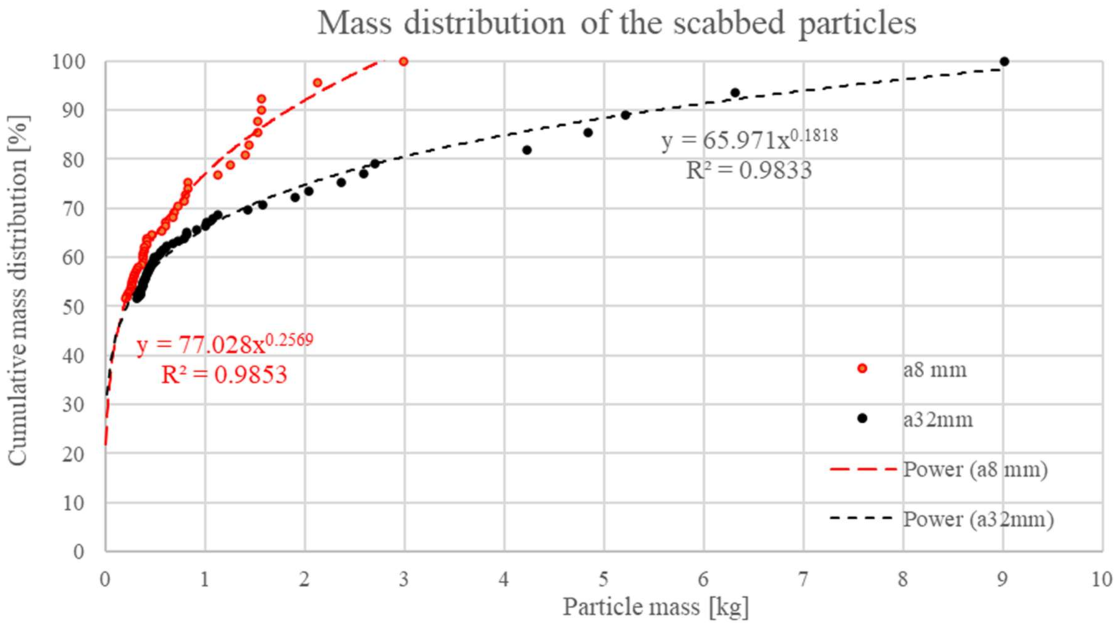

Figure 11. Mass distribution of the concrete particles detached from the tested slabs.

DISCUSSION AND CONCLUSIONS

The test results indicate that the grain size might have a larger effect on the punching resistance of concrete and thus also on the ballistic limit of concrete slabs than what could be expected based on the existing formulas. The tensile strength of concrete (as measured with splitting tensile strength) do not explain the results as the batches had comparable strength, even when higher loading velocities were used. There might be several reasons that contribute to the results of the executed tests. Part of the large and rather smooth aggregates became detached from the concrete matrix as single units instead of splitting in two. This requires less energy and thus provide less resistance against impact or shock load. The larger the grain size, the smaller the total cross-sectional area of the grains for the same mass of aggregates. This in turn results smaller resistance by the grains that are split during the impact. Since the tensile strength of granite is larger than that of the binders, this reduces the overall resistance of the slabs. Further tests, especially with reinforcement included, would be needed to confirm the findings.

REFERENCES

Orbovic, N., Sagals, G., Blahoianu, A. (2015). "Influence of transverse reinforcement on perforation resistance of reinforced concrete slabs under hard missile impact", *Nuclear Engineering and Design*, Vol. 295, pp. 716-729.

Kar, A.K. (1978). "Local effects of tornado generated missiles", *ASCE Journal of the Structural Division*, 104(ST5), pp. 809-816.

Kar, A. (1979). "Residual velocity for projectiles", *Nuclear Engineering and Design*, Vol. 53, pp. 87-95.

Tsiskreli, G.D., Dzhavakhidze, A.N.(1970)."The effect of aggregate size on strength and deformation of concrete", *Hydrotechnical Construction* **4**, 448–453 (1970). https://doi.org/10.1007/BF02376145

Whiffen, P. (1943). "UK road laboratory note no. MOS/311".